

Please cite the Published Version

Chohan, UK, Koehler, SPK and Jimenez-Melero, E (2017) Incipient FeO(1 1 1) monolayer formation during O-adsorption on Fe(1 1 0) surface. Computational Materials Science, 134. pp. 109-115. ISSN 0927-0256

DOI: <https://doi.org/10.1016/j.commatsci.2017.03.033>

Publisher: Elsevier

Version: Accepted Version

Downloaded from: <https://e-space.mmu.ac.uk/618755/>

Usage rights:



[Creative Commons: Attribution-Noncommercial-No Derivative Works 4.0](https://creativecommons.org/licenses/by-nc-nd/4.0/)

Additional Information: This is an Author Accepted Manuscript of a paper accepted for publication in Computational Materials Science, published by and copyright Elsevier.

Enquiries:

If you have questions about this document, contact openresearch@mmu.ac.uk. Please include the URL of the record in e-space. If you believe that your, or a third party's rights have been compromised through this document please see our Take Down policy (available from <https://www.mmu.ac.uk/library/using-the-library/policies-and-guidelines>)

Incipient FeO(111) monolayer formation during O-adsorption on Fe(110) surface

Urslaan K. Chohan^{a,c,}, Sven P. K. Koehler^{b,c,d}, Enrique Jimenez-Melero^{a,c}*

^aSchool of Materials, The University of Manchester, Manchester M13 9PL, UK

^bSchool of Chemistry, The University of Manchester, Manchester M13 9PL, UK

^cDalton Cumbrian Facility, The University of Manchester, Moor Row CA24 3HA, UK

^dPhoton Science Institute, The University of Manchester, Manchester M13 9PL, UK

*Corresponding author.

Email: urslaan.chohan@postgrad.manchester.ac.uk

University of Manchester

School of Materials

Oxford Road

Manchester

M13 9PL

United Kingdom

Abstract

The adsorption of O atoms on the Fe(110) surface has been investigated by density functional theory for increasing degrees of oxygen coverage from 0.25 to 1 monolayer, to follow the evolution of the O-Fe(110) system into an FeO(111)-like monolayer. We found that the quasi-threefold site is the most stable adsorption site for all coverages, with adsorption energies of ~ 2.8 to 4.0 eV per O atom. Oxygen adsorption results in surface geometrical changes such as interlayer relaxation and buckling, the latter of which decreases with coverage. The calculated vibrational frequencies range from 265-470 cm^{-1} for the frustrated translational modes and 480-620 cm^{-1} for the stretching mode, and hence are in good agreement with the experimental values reported for bulk FeO wüstite. The hybridization of the oxygen $2p$ and iron $3d$ orbitals increases with oxygen coverage, and the partial density of states for the O-Fe(110) system at full coverage resembles the one reported in the literature for bulk FeO. These results at full oxygen coverage point to the incipient formation of an FeO(111)-like monolayer that would eventually lead to the bulk FeO oxide layer.

Keywords: Density functional theory, ferrite, oxidation, chemisorption, partial density of states, surface relaxation

1. Introduction

The study of oxide formation on metallic surfaces is of great relevance in a wide range of technological applications, such as heterogeneous catalysis [1], oxide electronics [2] or nuclear reactor technologies [3]. In all these cases, the formation of an oxide on metallic surfaces is a sequential process. Initially, the surface exposure to oxygen results in the dissociative chemisorption of the oxygen molecules, resulting in a monolayer formation of oxygen atoms on the surface [4-6]. The metal surface atoms act as electron donors to these oxygen atoms [7]. With continuous exposure, this process eventually leads to the nucleation and growth of relatively thick surface oxide films. The incorporation and gradual diffusion of additional oxygen ions into the bulk structure, in parallel with the diffusion of metal cations from the bulk into the newly-formed oxide layer [5, 6, 8, 9], lead progressively to a compact bulk oxide [10]. It is important to note that an understanding of the initial O-chemisorption process and its transition into the surface oxide provides a first insight into the process of oxide formation in metallic systems.

In this study, we focussed on ferritic steels, which are present in various technological components where oxidation phenomena can compromise their structural integrity and limit their service life, such as in current power plants and potentially in advanced nuclear reactors concepts [11]. The low-index (110) plane of α -Fe is of particular interest, due to it being the most densely packed plane. The oxidation of this plane has been the subject of various studies through a plethora of methods, both theoretical and experimental, yet the initial stages of FeO formation are not yet fully understood. FeO wüstite is stable at temperatures above 570°C and can coexist with magnetite Fe₃O₄ at high oxygen levels [12, 13]. Linear kinetics has been reported for the oxidation of iron at low oxygen potentials where only FeO forms. The mobility of cations and electrons in FeO is relatively high [13]. As the wüstite scale thickens,

the diffusion rate through it decreases until a critical thickness is reached when diffusion becomes rate-controlling and the kinetics parabolic [12]. In this work we address the incipient formation of FeO from the initial oxygen chemisorption at the Fe(110) surface as the O-coverage increases, and before the FeO layer starts to grow and thicken.

There is significant scatter in the literature regarding the O-adsorption site and layer geometry for increasing coverage, and consequently regarding the vibrational frequencies for oxygen-covered iron, with a wide range of values measured, but not always with a clear assignment of the type of vibrational mode. A range of sticking coefficients for the adsorption of O₂ on Fe(110) were measured in various experiments, but later experiments were in agreement of a sticking coefficient of ~ 1 for low exposures, which decreased to ~ 0.05 for exposures close to 1 Langmuir (L) exposure [4, 14-16]. The earliest low energy electron diffraction (LEED) study investigated the mechanism of oxide layer formation on a single crystal of Fe(110) [17]. The (2 \times 2) and (3 \times 1) motifs were observed to form sequentially at 0.2 to 1.7 and 4 to 6 L, respectively. The authors also noted the formation of a FeO(111)-type structure at 18.5 L, which transitioned into a reconstructed quasi-hexagonal (5 \times 12) phase following an annealing step at 620 K. This sequence of formation was also observed by other groups [15, 18-20], although Weissenrieder et al. indicated the formation of an additional (2 \times 5) structure at low coverages [21]. In various studies the FeO(111) oxide layer was seen to form parallel to the Fe(110) surface, with a 4-6 % in-plane expansion in this oxide layer relative to bulk FeO [7, 22, 23]. Sakisaka et al. studied the band structure of the (2 \times 2) and (3 \times 1) structures using angle-resolved photoemission spectroscopy [24]. They found that the (2 \times 2) structure had negligible dispersion, however, the (3 \times 1)-O overlay exhibited a strong dispersion of ~ 1.6 eV, caused by O-Fe-O interactions. Spin- and angle-resolved photoemission and LEED experiments by Kim et al. agreed with that assignment [25]. A variety of studies employing a range of techniques were used to measure the Fe-O stretches

in FeO. An early investigation was conducted by Poling using transmission infrared spectroscopy on oxide powder samples. Two stretches were observed for FeO at $\sim 425\text{ cm}^{-1}$ and $\sim 580\text{ cm}^{-1}$ [26]. Erley and Ibach used high-resolution electron energy loss spectroscopy (HREELS) study to measure the vibrational frequencies of oxygen overlays for varying oxygen exposures [27]. They deduced that O atoms adsorb at long-bridge (lb) sites for low exposure, with a single vibration at around 500 cm^{-1} . The low frequency relative to a free O_2 molecule indicates that the O_2 undergoes dissociative chemisorption on the surface. After increasing the exposure, they observed an additional vibration at 200 cm^{-1} , correlating with a (2×2) oxygen overlay (0.50 ML). At still higher exposures, a (3×1) structure (0.67 ML) formed with O at lb sites, yielding vibrational stretches at $500\text{-}550\text{ cm}^{-1}$. At the highest exposures and following annealing at 750 K, the above mentioned (5×12) overlay formed, with stretches at 400 cm^{-1} and $500\text{-}550\text{ cm}^{-1}$, where the O atoms adsorbed at the quasi-threefold (3f) sites. Faria et al. used Raman spectroscopy to measure the Fe-O phonon interactions in pressed pellets of wüstite, and observed a broad peak at $\sim 652\text{ cm}^{-1}$ [28].

Theoretical calculations using density functional theory (DFT) of the adsorption of O atoms on the Fe(110) surface were first reported in the early 2000s. These DFT studies primarily investigated the (2×2) , (3×1) and (1×1) geometries [29-35]. There is consensus in the literature regarding the adsorption energy, which linearly increased from $\sim 1.40\text{ eV}$ to 3.50 eV per O atom from low to high coverage [30, 34]. However, there is disagreement regarding the stability of the four high symmetry adsorption sites (see Fig. 1). In the earlier studies, it was deduced that the most energetically stable adsorption site is the long-bridge (lb) site, while the on-top (ot), short-bridge (sb) and quasi-threefold (3f) sites were found to be unstable [29-31]. This was in contrast to a study by Błoński et al. in which the 3f site was found to be the most stable [32]. However, they attributed this to using a (3×3) geometry, unlike in the prior study which employed a (2×2) geometry. In a calculation by Tan, Zhou

and Peng, the authors assumed that the oxygen adsorbate resides at the lb site [33]. From their vibrational analysis, only the (2×2) and (3×1) structures were found to be stable. Most notably, they found the (1×1) structure to be a transition state. They did not comment upon this discrepancy beyond stating it is “not stable”, though this instability indicates that the oxygen atoms do not reside at the lb site at the highest coverage. Ossowski and Kiejna, however, indicated that for all coverages, the 3f site is most stable, with a small energy difference at low coverages between the lb and 3f sites [34]. Most recently, Freindl et al. conducted a combined DFT and experimental study [35]. They discovered a new (3×2) phase using LEED, corresponding to a 0.67 ML coverage, and verified its existence using DFT. The 3f site was found to be most stable for this structure.

In this work, we report an in-depth analysis into the adsorption of oxygen on the bcc Fe(110) surface with increasing coverages using density functional theory. The combined interpretation of the adsorption energies and vibrational frequencies allows to unequivocally determine the most stable adsorption site for representative degrees of coverage, and also to interpret the reported experimental values of vibrational frequencies. Changes in the spin-polarized partial density of states (PDOS) of oxygen adsorption on Fe(110), together with surface geometric effects due to adsorption such as interlayer spacing and buckling, are also discussed. This study considers a range of increasing O-coverage from 0.25 to 1 ML, hence we effectively probe the onset of oxidation up to the point where the calculated vibrational spectra and the partial density of states resemble those corresponding to FeO(111) films.

2. Computational methodology

Ab initio calculations were performed based on density-functional theory (DFT), using the Cambridge Serial Total Energy Package (CASTEP) electronic structure code [36]. The Perdew–Burke–Ernzerhof (PBE) framework described the exchange and correlation effects [37], and spin polarization was applied to accurately simulate the ferromagnetic

properties of α -Fe. CASTEP generated on-the-fly ultrasoft pseudopotentials for the Fe and O atoms. A slab model was used to represent a Fe(110) surface using six representative cell geometries; (2×2), (3×1), (2×1), (2×2)-2O, (3×1)-2O, and (1×1). Six layers and a vacuum gap of 20 Å were applied (see previous DFT study for further details [38]). The Monkhorst-Pack (MP) algorithm was employed for k point sampling [39]. A cut-off energy of 750 eV and 16×8×1 MP grid size yielded converged energies for the (2×1) geometry. The MP grid size was rescaled to apply consistent k point sampling for all geometries. The Gaussian smearing scheme was introduced to treat the partial occupancies about the Fermi level, with a smearing width of 0.1 eV [40]. Oxygen atoms were adsorbed to one side of the slab, with dipole effects considered negligible. Only the top three layers and the O atoms were relaxed, whilst the remaining three layers had their movement constrained. The Broyden–Fletcher–Goldfarb–Shanno (BFGS) algorithm [41] optimized the geometry, until the force per atom reached less than 0.05 eV/Å.

Two important surface parameters were calculated for the each employed slab geometry and O-adsorption site; the interlayer relaxation, Δ_{ij} and the adsorption energy, E_{ads} . The interlayer relaxation is given by

$$\Delta_{ij} = \left(\frac{d_{ij} - d_0}{d_0} \right) \times 100 \% \quad (1)$$

where d_0 is the bulk interlayer spacing and d_{ij} denotes the interlayer spacing between layers i and j in the slab. Values of Δ_{ij} were obtained for both the O-free and O-adsorbed Fe(110) surface. The adsorption energies were computed using the expression

$$E_{\text{ad}} = \frac{1}{N} \left[E_{\text{O+slab}} - \left(E_{\text{slab}} + \frac{N}{2} E_{\text{O}_2} \right) \right] \quad (2)$$

where $E_{\text{O+slab}}$ is the total energy of the O-covered slab, E_{slab} is the total energy of the clean slab, E_{O_2} is the energy of a free O₂ molecule (in a 10×10×10 Å³ box), and N is the number of

O adsorbates per unit cell. The relaxed geometries were carried forward into the frozen phonon calculations, to compute vibrational frequencies of the surface adsorbed O on high symmetry sites. The Fe slab atoms had constrained motion, whilst the O atoms were free to move. A finite displacement of 0.01 Å on O atoms was applied to compute the dynamical matrix, which was then implemented in calculating the vibrational frequencies.

The potential energy surface (PES) was calculated for the adsorption of oxygen on the Fe(110) plane. A grid was produced of 69 coordinate positions, which mapped the coordinates of O atoms along the surface. Three Fe substrate layers were allowed to relax, whilst fixing a single Fe atom on the top surface layer to limit surface reconstruction, and concurrently ensuring the energetics in the adsorption process were accurately captured. The O atom was allowed to relax normal to the plane only. The adsorption energy was calculated at each grid point, using Eq. 2. Energies were calculated relative to the energy at the ot site.

The spin-polarized partial density of states (PDOS), n^\pm , was calculated using the OPTADOS code [42]. Adaptive smearing was applied to smooth the PDOS, with a width of 0.4 eV [43]. From the PDOS, the spin-dependent d -band centre, c_d^\pm , was calculated via the relation [44]

$$c_d^\pm = \frac{\int_{-\infty}^{\infty} E n^\pm(E) dE}{\int_{-\infty}^{\infty} n^\pm(E) dE} \quad (3)$$

which was averaged to obtain the d -band centre, c_d , i.e. $c_d = 0.5(c_d^+ + c_d^-)$.

3. Results and Discussion

3.1. Stability of O-adsorption sites

We have calculated the adsorption energies of oxygen at the four potential sites on the Fe(110) surface for representative coverages using Eq. 2, see Fig. 2a. For all cell geometries, the lowest energy state is the 3f site, though for the (2×2) geometry (0.25 ML coverage), the 1b and 3f sites are close in energy. The sb and especially the ot sites are energetically less

favorable. These values suggest that the O atoms would preferentially adsorb on the 3f sites. As coverage increases, the adsorption energies decrease linearly. This reduction is likely to stem from an increasing repulsion between co-adsorbed O atoms with increasing coverage. The relative stability between adsorption sites is graphically presented on the potential energy surface plot for the (2×2) geometry, see Fig. 1. The ot and sb sites stand out as being energetically less favorable, but more importantly, it can be clearly seen that the lb and the 3f sites are not only very close in energy, but also very close spatially (~0.1 Å), with no discernible barrier between them.

After complete relaxation of the slab, the vibrational frequencies of the Fe–O bonds were computed using the frozen phonon method, see Table 1. An O atom was placed at all four possible adsorption sites for three representative cell geometries corresponding to 0.25, 0.5 and 1 ML, in order to observe the stability with respect to coverage. It can be seen that for all coverages, the sb and lb sites have a single imaginary frequency and are thus transition states. For 0.25 and 0.5 ML, the ot site is a rank two saddle point. For 1 ML coverage, the ot site is a local minimum, which accounts for the real frequencies at this coverage. However, the 3f site is a true minimum for all coverages, in agreement with our calculated adsorption energies. Only the 3f site as the most stable site will be considered in the following calculations.

3.2. Transition to FeO(111)-like monolayer

Vibrational frequencies were calculated for 0.25, 0.33, 0.5, 0.67 and 1 ML coverage for different cell geometries, see Table 2. For all coverages, at least three vibrations were observed, classified into two frustrated translational and one stretching mode. The frustrated translational frequencies, $\tilde{\nu}_{t1}$ and $\tilde{\nu}_{t2}$, oscillate parallel to the Fe(110) plane, whilst the stretching frequency, $\tilde{\nu}_s$ is normal to the plane, i.e. in the [110] direction. The frustrated translational mode $\tilde{\nu}_{t1}$ spans a frequency range from 265 to 465 cm⁻¹, oscillating in the $[\bar{1}\bar{1}0]$

direction, and the $\tilde{\nu}_{t2}$ mode from 375 to 470 cm^{-1} , oscillating in the [001] direction. Furthermore, the stretching frequency occurs at higher wavenumbers, i.e. between 480 cm^{-1} and 620 cm^{-1} . The relative increase in the frequencies for each mode correlates with the increasing coverage.

Fig. 2b shows the frequency values determined in our DFT work, and also the experimental values available in the literature for both oxygen adsorbed on Fe(110) surface and bulk FeO. Our calculated values for full coverage fit the early experiments by Poling et al. rather well [26]. They employed transmission IR spectroscopy of FeO powders, and hence observed what we believe are Fe–O stretches along the surface normal at $\sim 580 \text{ cm}^{-1}$ (as compared to our value of 620 cm^{-1} at full coverage), and also frustrated translational modes parallel to the surface at $\sim 425 \text{ cm}^{-1}$ (as compared to our 464 cm^{-1} and 466 cm^{-1} ; for reasons as to why one or two frequencies are detected, see discussion below) as these transmission IR studies were not restricted by the surface selection rules that limit reflection-absorption infrared spectroscopy studies on metal surfaces. The Raman studies by Faria et al. also detected a vibrational stretch at frequencies comparable to our results ($\sim 580 \text{ cm}^{-1}$ as compared to 620 cm^{-1}) [28]. In the HREELS work by Erley and Ibach [27], two oscillations for low O_2 exposure (corresponding to the (2×2) geometry) at 200 cm^{-1} and 500 cm^{-1} were observed. **As coverage increased, the 200 cm^{-1} stretch was no longer present, leaving a single 500 cm^{-1} stretch. Erley and Ibach argued that due to the EELS selection rule, namely that only stretching modes perpendicular to the surface are EELS active, the single stretch was necessary to be of at least C_{2v} symmetry [27]. From this it was concluded that the oxygen atom adsorbed at either the on-top or two-fold long-bridge site. However the stretching frequency is far away from that of a free FeO molecule (at $\sim 880 \text{ cm}^{-1}$) [45], and thus preference was given the 2f site for the adsorbed oxygen. Our analysis indicates that it is**

more likely that the O atoms occupy the 3f site. As has been mentioned earlier and as shown in Fig. 1, the 1b site and the 3f site are only separated by ~ 0.1 Å spatially, with the 3f site being surrounded by two potential 1b sites, and both sites are very close in energy ($\Delta E < 0.05$ eV at 0.25 ML coverage) as per our adsorption energy calculations, hence there is a probability that the O atom might migrate between the 1b and 3f sites. At increasing coverages, Erley and Ibach detected vibrations around $500\text{-}550\text{ cm}^{-1}$, which match our stretching frequencies well. This is an encouraging agreement as these studies were performed under specular HREELS conditions which are only sensitive to vibrations along the surface normal, which are stretching frequencies (but not the frustrated translation modes). An additional stretch at $\sim 400\text{ cm}^{-1}$ at the highest coverage and after annealing of the surface was believed to be due to the formation of FeO(111) after transitioning from a (5×12) geometry. This bilayer structure was found to have O atoms at the 3f sites with an increased Fe–O bond length, which seems to be responsible for the reduced vibrational frequency found in their study. Our results for O-coverage between 0.33 and 0.67 ML lie within the band of experimental values for oxygen adsorbed on the Fe(110) surface, while for full coverage our DFT values are in good agreement with the frequencies determined experimentally for bulk FeO, and therefore point to the formation of an FeO(111)-like monolayer at 1.0 ML.

The similarity between the calculated and experimentally observed vibrations for increasing O-coverage can be explained based on the calculated spin-polarized partial density of states (PDOS) of oxygen adsorption on Fe(110), see Fig. 3a-e. There is a shift in the density of states for the oxygen atoms, which is most noticeable in between -7 and -4 eV. Most notably, at the highest coverage, the form of the PDOS for the O atom begins to resemble the PDOS of the first layer of the Fe. This indicates there is hybridization between the $2p$ orbital of the O atom and the $3d$ orbital of the surface Fe atom. This is further

elaborated by calculating the d -band center, c_d , as a function of the adsorption energy, E_{ads} , see Fig. 3f. The linear relationship of the two parameters obeys the Hammer-Nørskov d -band model [46], which suggests that there is increasing hybridization with increasing coverage, and therefore the O atoms are becoming more strongly chemisorbed to the surface Fe atoms. This indicates that the surface layer is beginning to behave more like an oxide overlay at higher coverages. Furthermore, the form of the PDOS resembles those calculated in previous literature for FeO, in particular our calculated PDOS for low coverage is similar to the PDOS produced by Terakura et al. [47]. At high coverage there is resemblance to the PDOS produced by Ye et al. [48] and Rödl et al. [49], i.e. there is a peak alignment and similar form in the -4 to -7 eV range. Hence there are similarities in the electronic properties between FeO and our O-Fe(110) structures, especially at higher O-coverage.

3.3. Surface geometric effects from oxygen adsorption

The rearrangement of Fe atoms in the surface layers relative to the equilibrium bulk positions is a characteristic effect of the early stages of oxide formation, when the oxygen atoms become chemisorbed on the Fe(110) surface and the O-FeO(110) surface structure slowly evolve towards the occurrence of an oxide-like monolayer. The effect of adsorption is described in terms of the interlayer relaxation and buckling parameters, Δ_{ij} and b_i respectively. The interlayer relaxation was computed as a function of coverage in between the first and second layers, Δ_{12} , and second and third layers, Δ_{23} , as shown in Fig. 4a. We found that the first-to-second interlayer relaxation transitioned from negative (O-free surface) to positive for increasing O-coverage. Thus the adsorption of oxygen induces an expansion between the first two layers, relative to bulk Fe. The interlayer relaxation parameter shifts from $\Delta_{12} = -0.37\%$ for the O-free Fe(110) surface [38] to $\Delta_{12} = 2.02\%$ at 1 ML coverage. For coverages ranging $0 < \theta_{\text{O}} < 1$ ML, there is noticeable buckling in the first layer, b_1 , in the [110] direction induced by the O atoms bound at the 3f sites, as illustrated in Fig. 4b. The

oxygen atoms seem to be pushing the Fe atoms in the O-local environment on the (110) surface layer towards the bulk. At the lowest coverage, there is the greatest buckling at 0.08 Å. This value does not change rapidly with coverage, until we reach 1 ML for which there is no buckling present. This decrease and collapse in the buckling is expected as at the full monolayer coverage, the ‘pushing’ from the oxygen atoms is uniform throughout the surface, and therefore the buckling observed at lower degrees of O-coverage is suppressed for $\theta_0 = 1.0$ ML. There is a slight oscillation in the interlayer relaxation parameter in between the second and third layer, Δ_{23} , with respect to coverage. However, its value does not reveal a clear trend from clean to 1 ML coverage. It is likely that the small change in between these coverages is simply a compensatory effect from the shifting in the first two layers. This statement is supported by the negligible buckling observed in the second layer, b_2 , for all studied coverages. Thus it is clear that the adsorbed oxygen only strongly interacts with the first layer for an O-covered Fe(110) surface.

4. Conclusions

In this work, we have presented *ab initio* calculations simulating the early stages of oxidation on the (110) surface of bcc α -iron, namely the oxygen chemisorption and the incipient formation of an FeO(111)-like monolayer. We found the quasi-threefold 3f site to be most stable of all four high-symmetry adsorption sites for all O-coverages. For oxygen bound at the 3f site, adsorption energies range from ~ 2.8 to 4.0 eV per O atom for variable coverage. For low coverage, the quasi-threefold and the long-bridge (lb) sites are similar in energy, but the former becomes more favorable with increasing coverage. The short-bridge (sb) and on-top (ot) sites are highly unfavorable in terms of energy. This conclusion is re-enforced in the calculation of the vibrational frequencies, showing that the 3f site is a true minimum for all coverages, whilst the lb constitutes a transition state. The sb and ot are rank-two saddle points. The O-adsorption induces a relaxation of the first-to-second interlayer distance with

increasing coverage, and simultaneously a buckling effect in the first layer of the Fe(110) surface. The second and third layers are less sensitive to surface effects due to the O-adsorption. At full coverage the buckling in the first layer vanishes, while the relaxation parameter is highest. The analysis of the vibrational frequencies at full O-coverage yields values for the stretching and translational modes that are in good agreement with the experimental values for bulk FeO. This is supported by the increasing hybridization of the oxygen $2p$ and iron $3d$ orbitals with increasing oxygen coverage, and a close resemblance of the partial density of states for the O-Fe(110) system at full coverage with the one reported in the literature for bulk FeO. These results highlight the formation of an FeO(111)-like monolayer at full oxygen coverage, that will eventually lead to the bulk FeO surface oxide layer with increasing oxygen uptake and diffusion into the bulk.

Acknowledgements

We gratefully acknowledge the financial support of the Engineering and Physical Sciences Research Council UK (EPSRC) through the Centre for Doctoral Training in Advanced Metallic Systems. We also thank the Dalton Cumbrian Facility, partly funded by the Nuclear Decommissioning Authority, for providing funding to cover the cost of computational time.

References

- [1] Freund, H. and Pacchioni, G. (2008) Oxide ultra-thin films on metals: new materials for the design of supported metal catalysts. *Chem. Soc. Rev.* **37**(10) 2224-2242.
- [2] Ramesh, R. and Schlom, D. (2008) Whither oxide electronics? *MRS Bull.* **33**(11) 1006-1014.
- [3] Fox, K., Hoffman, E., Manjooran, N. and Pickrell, G. (2010) *Advances in Materials Science for Environmental and Nuclear Technology: Ceramic Transactions* John Wiley and Sons.
- [4] Dorfeld, W., Hudson, J. and Zuhr, R. (1976) The interaction of an O₂ molecular beam with an Fe (110) surface. *Surf. Sci.* **57**(2) 460-474.
- [5] Lawless, K. R. (1974) The oxidation of metals. *Rep. Prog. Phys.* **37**(2) 231-316.
- [6] Cabrera, N. and Mott, N. F. (1949) Theory of the oxidation of metals. *Rep. Prog. Phys.* **12**(1) 163-184.
- [7] Leygraf, C. and Ekelund, S. (1973) A LEED-AES study of the oxidation of Fe(110) and Fe(100). *Surf. Sci.* **40**(3) 609-635.
- [8] Williams, A. G. and Scherer, M. M. (2004) Spectroscopic evidence for Fe (II)-Fe (III) electron transfer at the iron oxide-water interface. *Environ. Sci. Technol.* **38**(18) 4782-4790.
- [9] Seybolt, A. U. (1963) Oxidation of metals. *Adv. Phys.* . **12**(45) 1-43.
- [10] Zhou, G. (2010) Nucleation-induced kinetic hindrance to the oxide formation during the initial oxidation of metals. *Phys. Rev. B.* **81**(19) 195440(1)-195440(7).
- [11] Klueh, R. L. (2009) Ferritic/martensitic steels for advanced nuclear reactors. *T. Indian I. Metals.* **62**(2) 81-87.
- [12] Young, D. (2008) *High temperature oxidation and corrosion of metals* Elsevier.
- [13] Birks, N., Meier, G. H. and Petti, F. S. (2006) *Introduction to the high temperature oxidation of metals* Cambridge University Press.
- [14] Pirug, G., Brodén, G. and Bonzel, H. P. (1980) Coadsorption of potassium and oxygen on Fe(110). *Surf. Sci.* **94**(2) 323-338
- [15] Miyano, T., Sakisaka, Y., Komeda, T. and Onchi, M. (1986) Electron energy-loss spectroscopy study of oxygen chemisorption and initial oxidation of Fe(110). *Surf. Sci.* **169**(1) 197-215.

- [16] Hodgson, A., Wight, A. and Worthy, G. (1994) The kinetics of O₂ dissociative chemisorption on Fe(110). *Surf. Sci.* **319**(1) 119-130.
- [17] Pignocco, A. J. and Pellissier, G. E. (1967) LEED studies of oxygen adsorption and oxide formation on an (011) iron surface. *Surf. Sci.* **7**(3) 261-278.
- [18] Wight, A., Condon, N. G., Leibslle, F. M., Worthy, G. and Hodgson, A. (1995) Initial stages of Fe(110) oxidation at 300 K: kinetics and structure. *Surf. Sci.* **331**(A) 133-137.
- [19] Smentkowski, V. S. and Yates, J. T. (1990) The adsorption of oxygen on Fe(110) in the temperature range of 90 to 920 K. *Surf. Sci.* **232**(1) 113-128.
- [20] Schüller, A., Busch, M., Seifert, J., Wethekam, S., Winter, H. and Gärtner, K. (2009) Superstructures of oxygen and sulphur on a Fe(110) surface via fast atom diffraction. *Phys. Rev. B.* **79**(23) 235425(1)-235425(15).
- [21] Weissenrieder, J., Göthelid, M., Månsson, M., von Schenck, H., Tjernberg, O. and Karlsson, U. O. (2003) Oxygen structures on Fe(110). *Surf. Sci.* **527**(1) 163-172.
- [22] Soldemo, M., Niu, Y., Zakharov, A., Lundgren, E. and Weissenrieder, J. (2015) A well-ordered surface oxide on Fe(110). *Surf. Sci.* **639** 13-19.
- [23] Busch, M., Gruyters, M. and Winter, H. (2006) FeO(111) formation by exposure of Fe(110) to atomic and molecular oxygen. *Surf. Sci.* **600**(13) 2778-2784.
- [24] Sakisaka, Y., Komeda, T., Miyano, T., Onchi, M., Masuda, S., Harada, Y., Yagi, K. and Kato, H. (1985) Angle-resolved photoemission of the c(2x2) and c(3x1) oxygen overlayers on Fe(110). *Surf. Sci.* **164**(1) 220-234.
- [25] Kim, H.-J. and Vescovo, E. (1998) Spin-resolved photoemission investigation of the c(2x2) and c(3x1) oxygen overlayers on the Fe(110) surface. *Phys. Rev. B.* **58**(20) 14047-14050.
- [26] Poling, G. W. (1969) Infrared Reflection Studies of the Oxidation of Copper and Iron. *J. Electrochem. Soc.* **116**(7) 958-963.
- [27] Erley, W. and Ibach, H. (1981) Vibrational excitations and structure of oxygen on Fe(110). *Solid State Commun.* **37**(12) 937-942.
- [28] de Faria, D. L. A., Silva, S. V. and de Oliveira, M. T. (1997) Raman Microspectroscopy of Some Iron Oxides and Oxyhydroxides. *J. Raman Spectrosc.* **28** 873-878.

- [29] Eder, M., Terakura, K. and Hafner, J. (2001) Initial stages of oxidation of (100) and (110) surfaces of iron caused by water. *Phys. Rev. B: Condens. Matter.* **64**(11) 1-7.
- [30] Błoński, P., Kiejna, A. and Hafner, J. (2005) Theoretical study of oxygen adsorption at the Fe(110) and (100) surfaces. *Surf. Sci.* **590**(1) 88-100.
- [31] Błoński, P., Kiejna, A. and Hafner, J. (2007) Oxygen adsorption on the clean and O precovered Fe(110) and (100) surfaces. *J. Phys.: Condens. Matter.* **19**(9) 1-8.
- [32] Błoński, P., Kiejna, A. and Hafner, J. (2008) Dissociative adsorption of O₂ molecules on O-precovered Fe(110) and Fe (100): Density-functional calculations. *Phys. Rev. B: Condens. Matter.* **77**(15) 1-8.
- [33] Tan, X., Zhou, J. and Peng, Y. (2012) First-principles study of oxygen adsorption on Fe(110) surface. *Appl. Surf. Sci.* **258**(22) 8484-8491.
- [34] Ossowski, T. and Kiejna, A. (2015) Oxygen adsorption on Fe(110) surface revisited. *Surf. Sci.* **637** 35-41.
- [35] Freindl, K., Ossowski, T., Zając, M., Spiridis, N., Wilgocka-Ślęzak, D., Madej, E., Giela, T., Kiejna, A. and Korecki, J. (2016) Oxygen Adsorption on the Fe (110) Surface: The Old System–New Structures. *J. Phys. Chem. C.* **120**(7) 3807-3813.
- [36] Clark, S. J., Matthew, I., Segall, D., Pickard, C. J., Hasnip, P. J., Probert, M. I. J., Refson, K. and Payne, M. C. (2005) First principles methods using CASTEP. *Z. Kristallogr.* **220** 567–570.
- [37] Perdew, J. P., Burke, K. and Ernzerhof, M. (1996) Generalized Gradient Approximation Made Simple. *Phys. Rev. Lett.* **77**(18) 3865-3868.
- [38] Chohan, U. K., Jimenez-Melero, E. and Koehler, S. P. K. (2016) Surface atomic relaxation and magnetism on hydrogen-adsorbed Fe (110) surfaces from first principles. *Appl. Surf. Sci.* **387** 385-392.
- [39] Pack, J. D. and Monkhorst, H. J. (1976) Special points for Brillouin-zone integrations. *Phys. Rev. B: Condens. Matter.* **13**(12) 5188-5192.
- [40] De Vita, A. (1992) The energetics of defects and impurities in metals and ionic materials from first principles. University of Keele.

- [41] Pfrommer, B. G., Côté, M., Louie, S. G. and Cohen, M. L. (1997) Relaxation of crystals with the quasi-Newton method. *J. Comput. Phys.* **131**(1) 233-240.
- [42] Morris, A., Nicholls, R., Pickard, C. and Yates, J. (2014) OptaDOS: A tool for obtaining density of states, core-level and optical spectra from electronic structure codes. *Comput. Phys. Commun.* **185**(5) 1477-1485.
- [43] Yates, J., Wang, X., Vanderbilt, D. and Souza, I. (2007) Spectral and Fermi surface properties from Wannier interpolation. *Phys. Rev. B.* **75**(19) 195121.
- [44] Kratzer, P., Hammer, B. and No, J. (1996) A theoretical study of CH₄ dissociation on pure and gold-alloyed Ni (111) surfaces. *J. Chem. Phys.* **105**(13) 5595-5604.
- [45] Stull, D. R. and Prophet, H. (1971) *JANAF thermochemical tables*.
- [46] Hammer, B. and Nørskov, J. (1995) Electronic factors determining the reactivity of metal surfaces. *Surf. Sci.* **343**(3) 211-220.
- [47] Terakura, K., T, O., Williams, A. and Kübler, J. (1984) Band theory of insulating transition-metal monoxides: Band-structure calculations. *Phys. Rev. B.* **30**(8) 4734-4747.
- [48] Ye, L., Asahi, R., Peng, L. and Freeman, A. (2012) Model GW study of the late transition metal monoxides. *J. Chem. Phys.* **137**(15) 186401(1)-186401(5).
- [49] Rödl, C., Fuchs, F., Furthmüller, J. and Bechstedt, F. (2009) Quasiparticle band structures of the antiferromagnetic transition-metal oxides MnO, FeO, CoO, and NiO. *Phys. Rev. B.* **79**(23) 235114(1)-235114(8).

Tables

Table 1. Wavenumbers of the Fe–O vibrations at the four studied adsorption sites on the Fe(110) surface, for representative cell geometries, with only one O atom adsorbed per cell. $\tilde{\nu}_{t1}$ and $\tilde{\nu}_{t2}$ are the frustrated translational modes, oscillating in the $[1\bar{1}0]$ and $[001]$ directions, respectively. $\tilde{\nu}_s$ is the stretching frequency, oscillating in the $[110]$ direction.

Cell geometry	Site type											
	3f			lb			sb			ot		
	$\tilde{\nu}/\text{cm}^{-1}$											
	$\tilde{\nu}_{t1}$	$\tilde{\nu}_{t2}$	$\tilde{\nu}_s$	$\tilde{\nu}_{t1}$	$\tilde{\nu}_{t2}$	$\tilde{\nu}_s$	$\tilde{\nu}_{t1}$	$\tilde{\nu}_{t2}$	$\tilde{\nu}_s$	$\tilde{\nu}_{t1}$	$\tilde{\nu}_{t2}$	$\tilde{\nu}_s$
(1×1)	464	466	620	221i	414	456	179i	454	593	174	205	785
(2×1)	341	386	531	156i	448	518	165i	404	596	178i	73i	752
(2×2)	265	371	481	40i	453	456	163i	420	566	146i	129i	741

Table 2. Wavenumbers of the Fe–O vibrations for oxygen located at the 3f adsorption site, for all studied combinations of cell geometries and coverages (θ_o).

Cell geometry	θ_o/ML	$\tilde{\nu}/\text{cm}^{-1}$		
		$\tilde{\nu}_{t1}$	$\tilde{\nu}_{t2}$	$\tilde{\nu}_s$
(2×2)	0.25	265	371	481
(3×1)	0.33	351	380	521
(2×1)	0.50	341	386	531
(2×2)-2O	0.50	313/339	393/426	501/530
(3×1)-2O	0.67	331/408	410/419	521/558
(1×1)	1.00	464	466	620

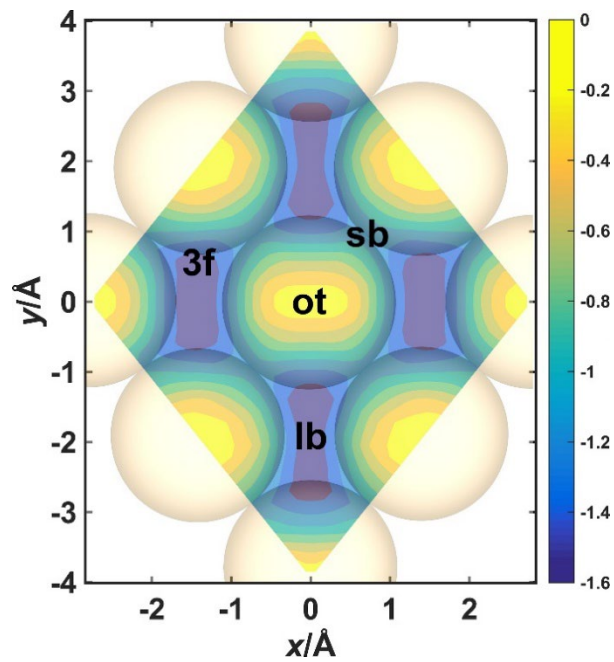


Figure 1. The potential energy surface for oxygen adsorbed on the Fe(110) surface, at and in between the various high symmetry adsorption sites. The adsorption sites for O atoms on the Fe(110) plane are depicted as follows: the quasi-threefold (3f), long-bridge (lb), short-bridge (sb), and on-top (ot) sites. The (2×2) geometry was selected to generate the potential energy surface.

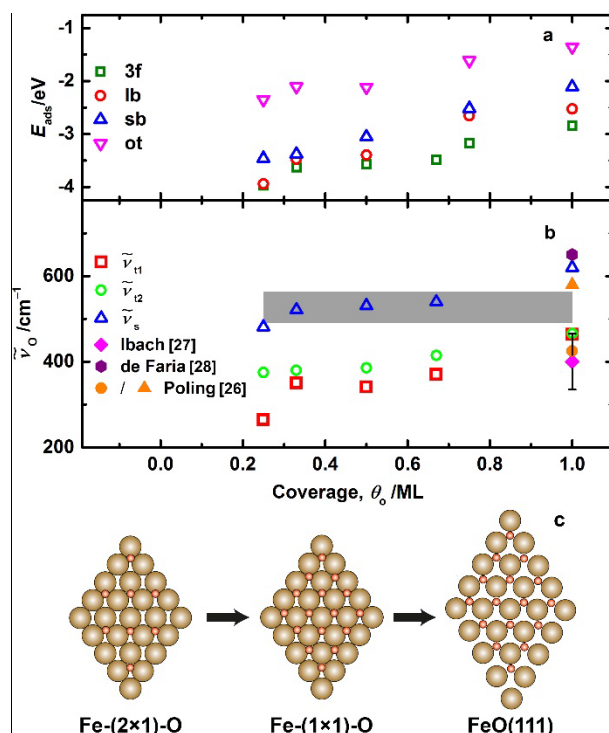


Figure 2. (a) Calculated adsorption energies at four high symmetry adsorption sites, and (b) vibrational frequencies at the 3f site for O adsorbed on Fe(110) at various coverages. Closed symbols depict the experimental values from previous experimental work. The grey band depicts the range of vibrational frequencies for varying coverages of adsorbed oxygen as measured by HREEL in Ref. [27]. (c) The surface arrangements for half and full monolayer oxygen coverage, and the arrangement of atoms to form the FeO(111) monolayer.

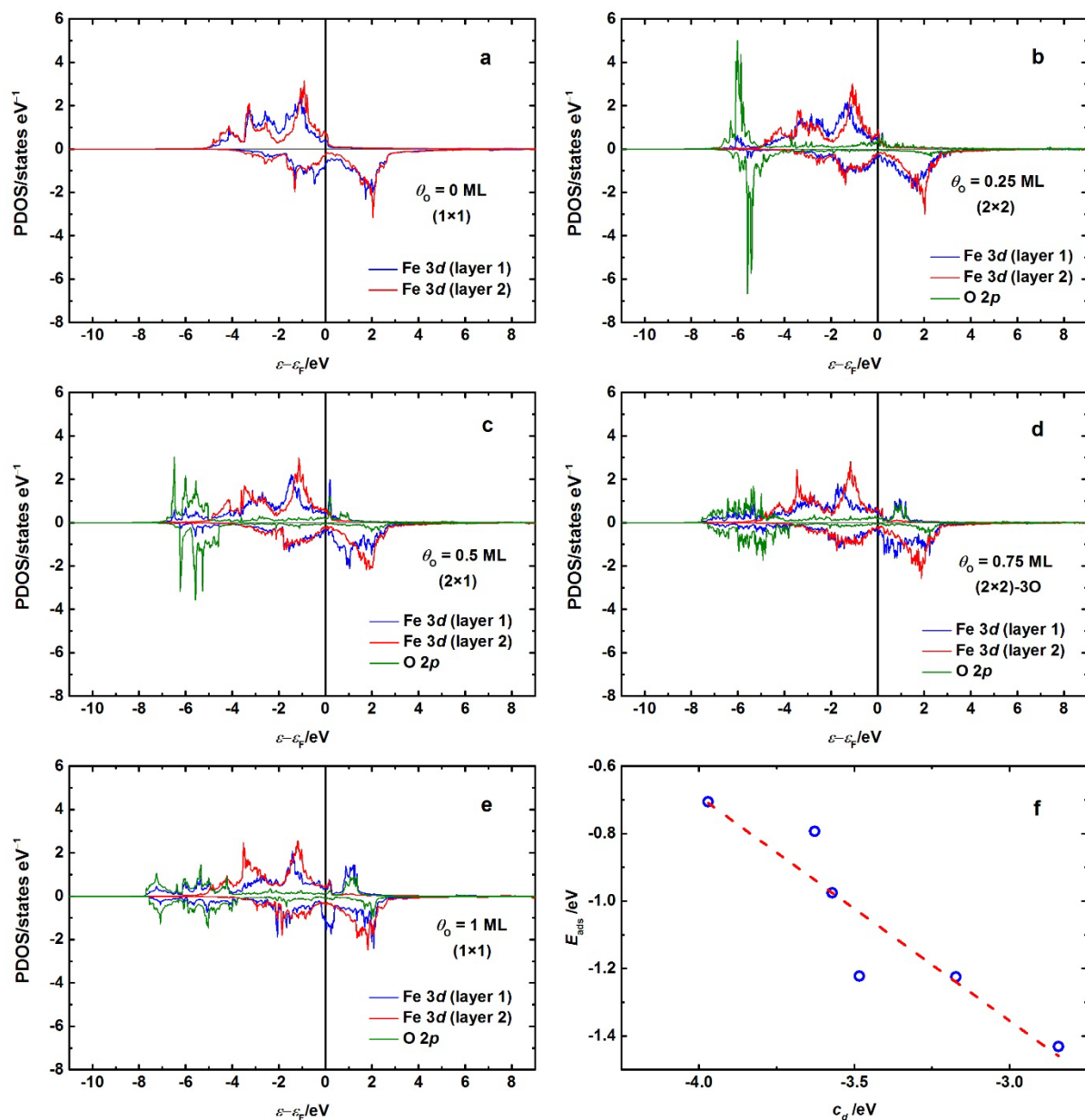


Figure 3. (a)-(e) Spin-polarized partial density of states (PDOS) of oxygen adsorption on Fe(110) at the i th layer ($i=1,2$) for increasing coverage; from 0-1 ML (in 0.25 ML intervals). The vertical line denotes the Fermi energy, E_F . (f) Adsorption energy, E_{ads} , as a function of the d -band center, c_d , the latter calculated from the PDOS. The dashed line is a guide to the eye.

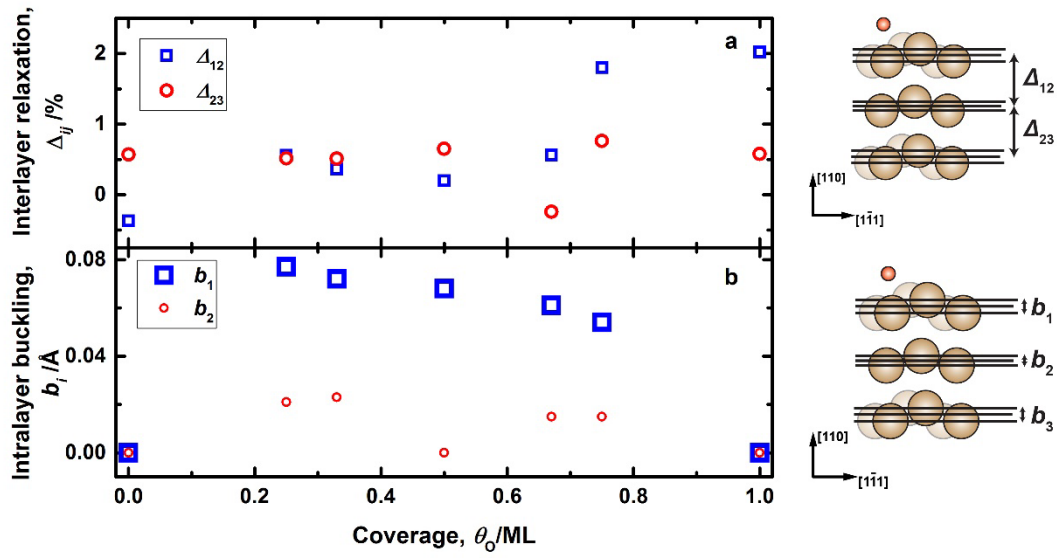


Figure 4. (a) The interlayer relaxation Δ_{ij} between layers i and j of the Fe(110) surface, together with (b) intralayer buckling b_i , as a function of coverage.